Journal of Environmental Management 326 (2023) 116816

Contents lists available at ScienceDirect

Journal of Environmental Management

journal homepage: www.elsevier.com/locate/jenvman

Research article

Hydrological connectivity affects nitrogen migration and retention in the land–river continuum

Yao Wang [a,b], Jingjie Lin [a,b], Fenfang Wang [a,b], Qing Tian [a,b], Yi Zheng [c], Nengwang Chen [a,b,*]

[a] Fujian Provincial Key Laboratory for Coastal Ecology and Environmental Studies, College of the Environment and Ecology, Xiamen University, Xiamen, China
[b] State Key Laboratory of Marine Environmental Science, Xiamen University, Xiamen, China
[c] School of Environmental Science and Engineering, Southern University of Science and Technology, Shenzhen, China

ARTICLE INFO

Keywords:
Hydrologically sensitive areas
Land use
Nitrification and denitrification
Water quality
Watershed management

ABSTRACT

Land use change and excessive nitrogen (N) loading threaten the health of receiving water bodies worldwide. However, the role of hydrological connectivity in linking watershed land use, N biogeochemistry and river water quality remain unclear. In this study, we investigated 15 subwatersheds in the Jiulong River watershed (southeastern China) during a dry baseflow period in 2018, combined with 3–year (2017–2019) nutrient monitoring in 5 subwatersheds to explore river N dynamics (dissolved nutrients, dissolved gases and functional genes) and their controlling factors at three hydrological connectivity scales, i.e., watershed, hydrologically sensitive areas (HSAs) and riparian zone. The results show that land use at HSAs (less than 20% of watershed area) and watershed scales contributed similarly to river N variation, indicating that HSAs are hotspots for transporting land N into river channels. In particular, the agricultural land was the main factor affecting river nitrate and nitrous oxide (N_2O) concentrations, while the built–up land significantly affected river ammonium and nitrite. At the riparian zone scale, soils and sediments substantially influenced river N retention processes (i.e., nitrification and denitrification). Management and protection measures targeting HSAs and riparian zones are expected to efficiently reduce river N loading and improve water quality.

1. Introduction

Nitrogen (N) is the foundation on which life forms depend, and its cycle is one of the most important biogeochemical processes that affect the aquatic environment (Lutz et al., 2020; Zhu et al., 2021). However, intensive human activities have released excess N into the soil and water environments and finally caused the deterioration of river quality (Lehnert et al., 2021; Lin et al., 2020a; Shrewsbury et al., 2016; van–Lent et al., 2015). In particular, the changes in land use/cover (e.g., intensive agriculture and rapid urbanization) are a comprehensive reflection of human activities and perturbed nutrient balances at the watershed scale, which may eventually impact the sustainability of aquatic ecosystems and human systems (Giri et al., 2018; Song et al., 2018). In addition, recent studies have shown that land use management at the riparian zone scale strongly affects river quality (Fox et al., 2016; Hansen et al., 2021; Zaimes et al., 2021). Riparian erosion is considered as a significant source of material to rivers, which contributes 21%–24% of the total N loads (Willett et al., 2012) and 7%–92% of the suspended sediment loads (Fox et al., 2016). This could dramatically alter the N cycle in river systems. Therefore, understanding the impacts of land use on the migration and transformation of N at different scales is essential for developing management strategies in regard to watershed nutrients to improve water quality and mitigate eutrophication.

However, it is uneconomical and impractical to enforce protective management on all land in a watershed. Critical source areas (CSAs) have been considered areas with the greatest risk of pollutant transfer at the watershed scale (Walter et al., 2000). Identification of CSAs is helpful for nutrient management and restoration of aquatic ecosystems. The main method for identifying CSAs is spatial modeling using geomorphological and hydrological information (e.g., soil and water assessment tool). However, the modeling process is long and complex (Li et al., 2021). Some studies have also shown that CSAs fall short in defining the transport capacity of pollutants by surface runoff (Giri et al., 2017; Thomas et al., 2016). This is mainly because CSAs are usually presented by polygons, while overland flow tends to channelize and converge due to terrain (Giri et al., 2018; Qiu et al., 2019; Thomas et al.,

* Corresponding author. Fujian Provincial Key Laboratory for Coastal Ecology and Environmental Studies, College of the Environment and Ecology, Xiamen University, Xiamen, China.
E-mail address: nwchen@xmu.edu.cn (N. Chen).

https://doi.org/10.1016/j.jenvman.2022.116816
Received 24 March 2022; Received in revised form 28 September 2022; Accepted 14 November 2022

2017). Thomas et al. (2016) pointed out that to determine CSAs with diffuse pollution in agricultural watersheds, it is necessary to accurately determine hydrologically sensitive areas (HSAs).

HSAs are areas with a high propensity for generating runoff and transporting pollutants to rivers in a watershed (Qiu et al., 2019; Walter et al., 2000). They can comprehensively take into account among saturation–and–infiltration–excess mechanisms of overland flow generation, the concept of hydrological connectivity regarding transport pollutants, and the location of CSAs (Agnew et al., 2006; Thomas et al., 2016). HSAs occupy a small area in the watershed, and the best management practices implemented in HSAs are a more ideal and effective way to reduce management investment and to improve the quality of aquatic ecosystems. Studies in recent years have shown that identifying HSAs has been recognized as an effective way to estimate soil moisture patterns (Buchanan et al., 2014), develop water quality management strategies (Giri et al., 2017) and assess the degradation of aquatic ecosystems (Qiu et al., 2019). However, the role of HSAs in regulating N migration and cycling along the land–river continuum remains unclear. In particular, the riparian zone is regarded as the last line of defense against pollutants entering rivers (Anderson et al., 2015; Lutz et al., 2020; Zhao et al., 2021). HSAs transfer nutrients to the river across the riparian zone, which may dramatically alter the N cycle (e.g., nitrification and denitrification) of the river.

Nitrification and denitrification are the two most important N cycle processes and are critical measures of ecological restoration of rivers (Lin et al., 2020a). In watersheds, river ammonium (NH_4–N) pollution can be reduced through the nitrification process, and total N pollution can be reduced through the denitrification process (Lehnert et al., 2021; Lin et al., 2020b; Zhao et al., 2021). Generally, nitrification is the process of converting NH_4–N to nitrite (NO_2–N) and then to nitrate (NO_3–N), which is performed by ammonia–oxidizing archaea (*amo*A–AOA) and bacteria (*amo*A–AOB) and nitrite–oxidizing bacteria (e.g., *nxr*A) (Bossolani et al., 2020; Tang et al., 2019). Denitrification refers to the process of converting NO_3–N to NO_2–N and nitric oxide (NO) and then to nitrous oxide (N_2O) and dinitrogen (N_2) by denitrifiers (e.g., *nar*G and *nir*S) (Abbas et al., 2020; Lutz et al., 2020). Land uses and environmental components (e.g., soils, river water, and sediments) have strong effects on river nitrification and denitrification (Giri et al., 2018; Shrewsbury et al., 2016; van–Lent et al., 2015). In particular, the agricultural fertilization and domestic sewage converge to river channels under the effect of hydrological connectivity, which may change the river N cycle. However, the main controlling factors and mechanisms regarding river nitrification and denitrification in hydrological connectivity are still unclear.

In this study, we investigated 15 subwatersheds, combined with 3–year nutrient monitoring in 5 subwatersheds, identified their land use patterns, delineated HSAs, and analyzed N dynamics (dissolved N, N_2O, N_2 and functional genes) in the soils, river water and sediments. The specific objectives of this study were to (1) compare the effects of land use on river N dynamics at the watershed and HSAs scales, and (2) reveal the important processes controlling river N retention at the riparian zone scale. The relationships between land use, hydrological connectivity and river N and associated implications for watershed nutrient management were discussed.

2. Materials and methods

2.1. Study area

The Jiulong River is a subtropical river located in Fujian Province, southeastern China (Fig. 1). The Jiulong River has a drainage area of 14,740 km^2, which consists of two major tributaries, including the North Jiulong River (NJR) and West Jiulong River (WJR) (Chen et al., 2015). In this region, the annual rainfall is 1436 ± 10 mm during 2017–2019 based on four weather station (ZP, CT, NJ and ZZ), and ~75% occurs in the wet season (April to September). The annual mean flow of NJR (PN

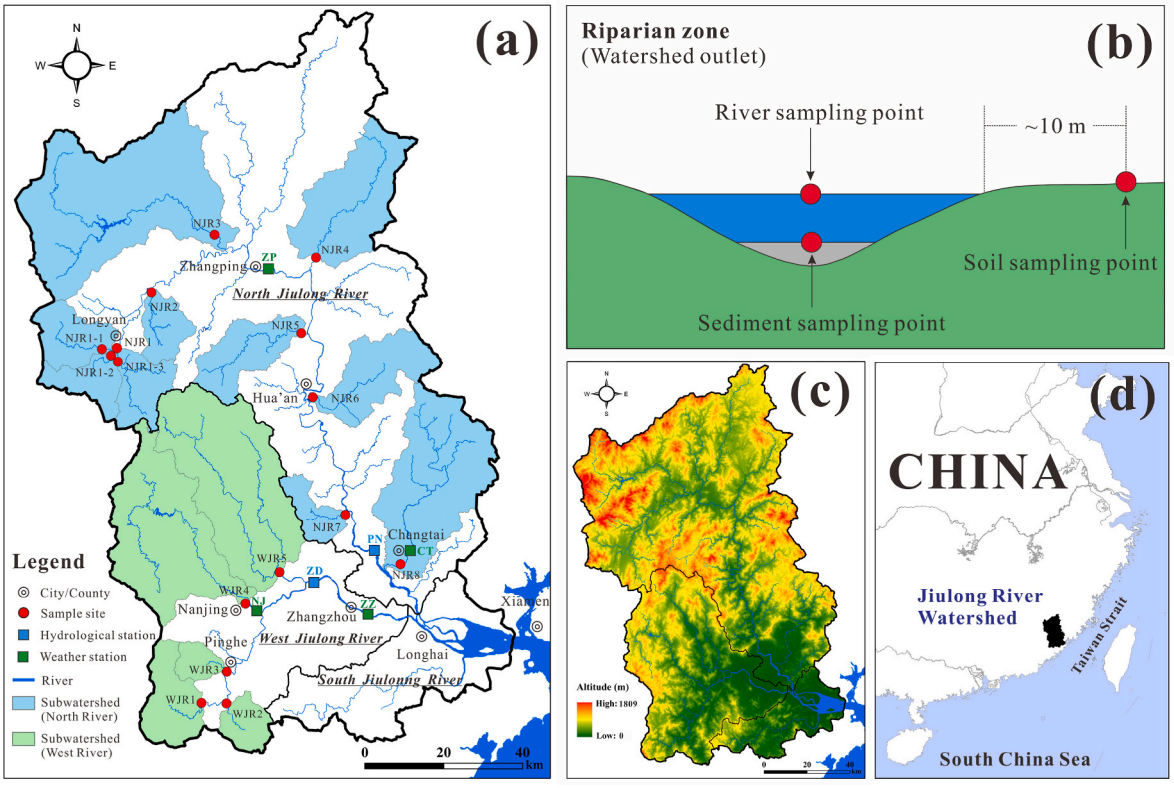

Fig. 1. The spatial distribution of 15 subwatersheds in the Jiulong River watershed (a), the distribution of sampling sites in riparian zone of subwatershed outlet (b), watershed altitude (c) and the location of study area (d).

hydrological station) and WJR (ZD hydrological station) is 228 ± 61 and 83 ± 26 m^3 s^{-1} during 2017–2019, respectively. Detailed monthly variations in rainfall and flow can be found in Fig. S1. The mean values of the slope in the NJR and WJR watersheds were 20.2° and 17.3°, respectively. Areas of slope >25° accounted for 31.8% and 24.1% of the total area in the NJR and WJR watersheds, respectively. In the present study, considering no water transfer across the watershed boundary, a total of 15 subwatersheds (10 in the NJR watershed and 5 in the WJR watershed) were selected to explore the effects of land use, sediments and riparian soils on river N (Fig. 1). Details of the 15 subwatersheds can be found in Table S1. The major land uses include agricultural land, built−up land and natural land in the Jiulong River watershed (Lin et al., 2020b). The spatial distribution of land uses in 2018 is presented in Fig. S2. Especially in agricultural land, the main crop types including Tea, Peanuts, Lichi, Seedling, Vegetables, Paddy, Banana, Pomelo and Corn (Xiong et al., 2022). Monthly fertilization schedule for each crop in agricultural land was shown in Table S2.

2.2. Sampling campaign

In this study, a total of 41 sample stations for river water (n = 15), sediments (n = 15), and riparian soils (n = 11) were placed near the outlet of 15 subwatersheds in the Jiulong River watershed in November of 2018.

River water (0.5 m) was collected using a 5 L polymethyl methacrylate hydrophore. Water was carefully introduced into the bottom of 60 mL (N_2O) and 12 mL (N_2) sample bottles using a silicone tube for dissolved gas analyses. After the water overflowed by twice the volume of the sample bottle, a final concentration of 0.1% $HgCl_2$ was added to stop microbial activity. The cap was tightened immediately to ensure that there were no bubbles at the top of the sample bottle. Duplicate samples were prepared and stored in a cooler containing freshwater to maintain temperature. Meanwhile, approximately 1 L water was filtered by a GF/F membrane for total suspended matter (TSM), and the filtrate was used for nutrient analysis. To quantify the abundance of river N functional genes, 1 L water was filtered through a 20 μm bluteau and followed by 0.22 μm Isopore Membrane Filters (47 mm, Millipore, USA). The GF/F membrane and filtrate were immediately processed for TSM and nutrient analysis upon arrival at the laboratory. Isopore membrane filters were stored in a −80 °C freezer until DNA extraction.

Surface sediments (0–5 cm) were collected at the central axis of the river by a stainless grab. Previous studies have shown that a 5–30 m riparian buffer width is beneficial for water quality protection; in particular, most filtering occurs within the first 10 m for low−moderate slope (Fischer and Fischenich, 2000). Therefore, soil samples (0–20 cm) were collected at a distance of ~10 m from the river (i.e., riparian zone width). Each soil sample was a mixture of five soil profiles within a 20 m^2 plot. A total of approximately 200 g sediments and 500 g soils were placed on ice and transported to the laboratory. Upon arrival at the laboratory, the sediment and soil samples were immediately processed for analysis of physicochemical properties. A small fraction (approximately 50 g) of the sediment and soil samples was stored in a −80 °C freezer for subsequent molecular analysis to quantify the abundance of the N functional genes.

To further assess the relationship between land use and river N at the watershed and HSAs scales across time, the seasonal dynamics of N (NO_3–N, NO_2–N and NH_4–N) were collected at 5 long−term monitoring stations of NJR1, WJR1, WJR3, WJR4 and WJR5 during 2017–2019 (month/day/year: 7/27/2017, 11/12/2017, 1/9/2018, 4/21/2018, 7/20/2018, 11/11/2018, 2/18/2019, 4/23/2019, 7/1/2019 and 11/24/2019) (Fig. 1 and S1).

2.3. Physicochemical analysis

Water temperature, conductivity, dissolved oxygen (DO) and pH were measured in situ by a WTW multiparameter portable meter (Multi 3430, Germany). The filtered GF/F membranes were heated in an oven at 105 ± 2 °C until a constant weight. TSM was calculated as the difference in weight between the unfiltered and filtered GF/F membranes. The concentrations of NO_3–N, NO_2–N and NH_4–N were determined using segmented flow automated colorimetry (San++ analyzer, Germany). Dissolved inorganic N (DIN) was the sum of NO_3–N, NO_2–N and NH_4–N. Dissolved total N (DTN) was determined as NO_3–N following oxidization with 4% alkaline potassium persulfate. Dissolved organic N (DON) was calculated as the difference between DTN and DIN. The precision of the N components was determined by repeated 10% samples, and the relative error was less than 5%. The concentration of dissolved N_2O was determined by gas chromatography (Agilent 7890A, US). The concentration of dissolved N_2 was measured using the N_2:Ar ratio method by membrane inlet mass spectrometry (MIMS). Excess dissolved N_2O (ΔN_2O) and N_2 (ΔN_2) were calculated by the method described in Chen et al. (2014). Seasonal river sampling only measured dissolved nutrients.

Sediment and soil samples were placed in aluminum boxes and heated in an oven for 24 h at 105 ± 2 °C to obtain their water content. The pH of the sediment and soil was measured using a pH meter after suspending the soil solution at a soil−water ratio of 1:5. The NO_3–N, NO_2–N and NH_4–N contents of sediment and soil were determined using segmented flow automated colorimetry after extraction by 2 mol L^{-1} KCl.

2.4. Molecular analysis of nitrogen functional genes

DNA was extracted from isopore membrane filters, sediments and soils using the FastDNA Spin Kit for Soil (MP Biomedicals, Solon, OH, USA). A NanoDrop spectrophotometer (DN−1000; Isogen Life Science, the Netherlands) was used to detect the concentration and purity of DNA samples. Nitrifying genes include *amo*A−AOA, *amo*A−AOB and *nxr*A. Denitrifying genes include *nar*G and *nir*S. The primers were Arch−*amo*AF/Arch−*amo*AR (*amo*A−AOA), *amo*A2F/*amo*A2R (*amo*A−AOB), F1370–F1/F2843−R2 (*nxr*A), 1960m2f/2050m2r (*nar*G) and cd3Af/R3cd (*nir*S). Bio−Rad CFX96 qPCR was used to quantify the abundance of these genes in triplicate with three negative controls (no DNA template) and five standards. Each sample had 10 μL of Hieff qPCR SYBR Green Master Mix (Yeasen, China), 0.4 × 2 μL of primers, 1 μL of template DNA and 8.2 μL of double−distilled H_2O added. The detailed methods of the primers and qPCR amplification were given by Lin et al. (2020b).

2.5. Soil topographic index

The soil topographic index (STI) method is commonly used to identify HSAs, and can consider both the spatial variability and hydrological connectivity of the landscape to estimate the runoff−contributing areas (Anderson et al., 2014; Giri et al., 2018; Qiu et al., 2019). The STI can be calculated by Equation (1) (Buchanan et al., 2014).

$$\mathrm{STI} = \ln(\alpha / \tan\beta) - \ln(\mathrm{Ks} \times \mathrm{D}) \quad (1)$$

where $\ln(\alpha/\tan\beta)$ is the topographic wetness index (TWI), which indicates the distribution of soil properties and soil moisture at different landscape positions. Specifically, α is the upslope−contributing area per unit contour length (m), and β is the topographic slope (mm^{-1}). The upslope−contributing area and slope were derived from a digital elevation model (DEM) at 12.5 m resolution from Advanced Land Observation Satellite−Phased Array Type L−band Synthetic Aperture Radar (ALOS−PALSAR) (https://search.asf.alaska.edu/#/). $\ln(\mathrm{Ks} \times \mathrm{D})$ is the soil transmissivity, Ks is the saturated hydraulic conductivity (m d^{-1}), and D is the soil depth above the restrictive layer (m). Ks for different soil types were calculated based on soil particle size and soil organic matter in SPAW Hydrology software (version 6.02.75). The data of soil particle size, soil organic matter and D in different soil types from

Fujian Provincial Soil Survey Office (Lin, 1991). The calculation process of STI is completed in ArcGis software (version 10.2).

2.6. Hydrologically sensitive areas

Usually, a prior STI threshold was selected, and the region whose STI value was greater than the threshold was considered HSAs (Buchanan et al., 2014; Giri et al., 2018). The higher the threshold was, the smaller the area of the HSAs. Giri et al. (2017) identified the range of STI values from 9 to 15 for delineating HSAs based on field soil moisture data and a polynomial regression model of order 2 to 4. Giri et al. (2018) further assessed the impacts of land uses with HSAs on water quality by applying a STI threshold value of 10 at a larger scale: north–central New Jersey watersheds, USA. Qiu et al. (2019) used a STI value of 10 to assess the relationship between landscape alteration and aquatic ecosystem degradation. According to previous studies, a STI threshold value of 10 was chosen to delineate HSAs in this study. The spatial distribution of HSAs is presented in Fig. 2.

2.7. Statistical model analysis

In this study, the parameters regarding N were classified as dissolved nutrients (DTN, DON, DIN, NO_3–N, NO_2–N and NH_4–N), dissolved gases (ΔN_2 and ΔN_2O), nitrifier genes (*amo*A–AOA, *amo*A–AOB and *nxr*A) and denitrifier genes (*nar*G and *nir*S). Three main scales were considered, including watershed, HSAs and riparian zone scales.

At the watershed and HSAs scales, multiple linear regression (MLR) analysis was conducted to determine the relationship between land use and river N across space and time. Here, only one set of water quality data (sampling at central river in watershed outlet, Fig. 1b), but which was established in the regression relationship with land use at watershed scale and HSAs scale, respectively. Considering the comparability of the MLR model at different scales, the land use and river N data were transformed by the logarithmic method before MLR analysis. For MLR analysis, a stepwise regression method was selected because of its advantages in simplifying the equation, speeding up modeling, containing only significant variables and avoiding the multicollinearity problem (Wang et al., 2021). In addition, the adjusted determination coefficient (adjusted R^2), Akaike information criterion (AIC) and Bayesian information criterion (BIC) as model evaluation parameters were used to determine the predictive performance of land use on river N at both watershed and HSAs scales. In particular, AIC can consider both goodness–of–fit and degree of freedom, which is regarded as the optimal method to evaluate the model (Hurvich et al., 1998). The optimal model was determined based on higher adjusted R^2 values and lower AIC and BIC values.

The T–test was used to assess the differences in soil/river/sediment N between the NJR and WJR. Redundancy analysis (RDA), a multivariate direct gradient analytical method, not only reflects the correlation among samples, nutrients and environmental factors, but also reveals the factors with a greater degree of influence. In this study, RDA was used to reveal the relationships between environmental factors and river N at watershed and HSAs scales (Fig. S3) and riparian zone scale (Fig. S4). The contribution of the significant environmental factors to river N (dissolved nutrients, dissolved gases, nitrifier and denitrifier genes) at different scales quantified with RDA resluts, which were summarized in Section 3.4. The RDA was performed in Canoco software (version 5.0). The statistical significance was tested by the Monte Carlo permutation method based on 499 runs with randomized data.

3. Results

3.1. Hydrologically sensitive areas and land use

The STI value ranged from 0.4 to 31.6 for the entire Jiulong River watershed (Fig. 2). HSAs accounted for 13.3% of the total area of the Jiulong River watershed (Table S1). Specifically, HSAs accounted for 8.0%–17.3% and 13.7%–17.0% of each subwatershed area in the NJR (n = 10) and the WJR (n = 5) watersheds, respectively.

The percentage of typical land uses at both watershed and HSAs scales is shown in Fig. 3. For all subwatersheds (n = 15), natural land had the highest proportion (more than 50%) at both watershed and HSAs scales, followed by agricultural land (more than 20%) and built–up land (less than 15%). At the watershed and HSAs scales, compared with the NJR watershed, the WJR watershed had a lower proportion of built–up land and natural land and a higher proportion of agricultural land.

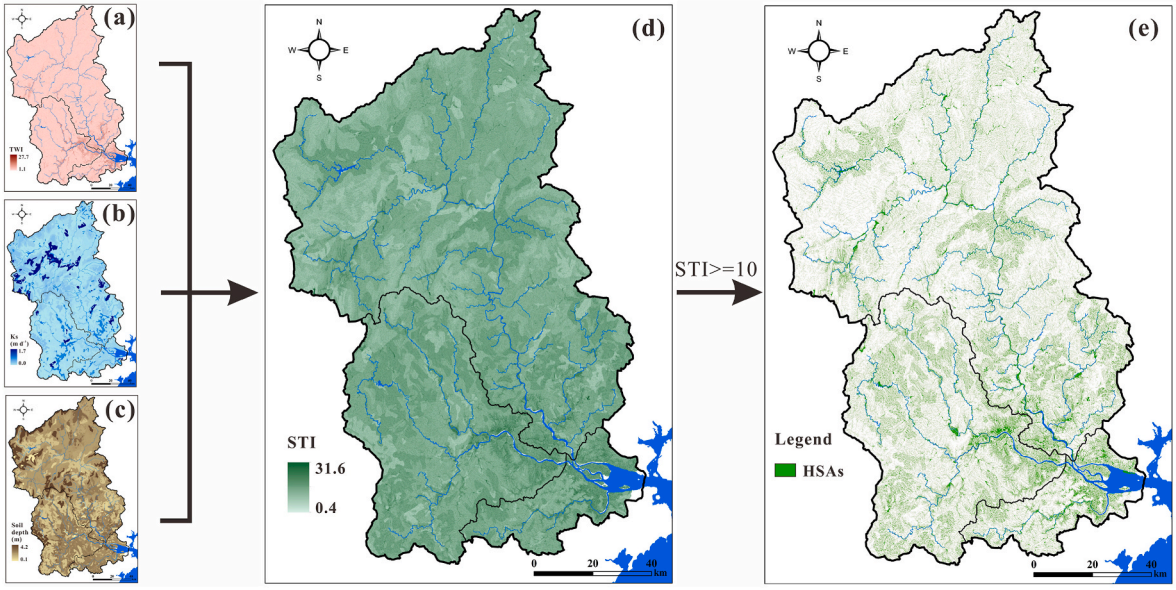

Fig. 2. The spatial distribution of topographic wetness index (TWI) (a), saturated hydraulic conductivity (Ks) (b), soil depth (c), soil topographic index (STI) (d), and hydrologically sensitive areas (HSAs) (e) in the Jiulong River watershed.

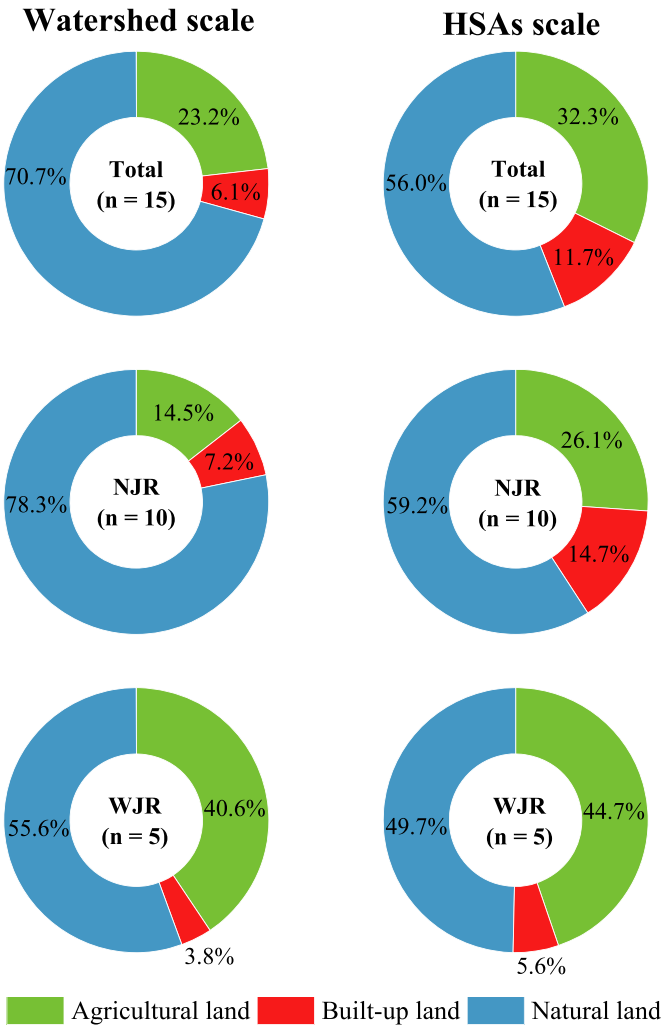

Fig. 3. Percentages of land uses for total subwatersheds, North Jiulong River (NJR) subwatersheds and West Jiulong River (WJR) subwatersheds at the watershed and HSAs (hydrologically sensitive areas) scales.

3.2. Physicochemical characteristics of the soil, river and sediment

The physicochemical characteristics of the soil, river and sediment are presented in Table 1. For all subwatersheds (n = 15), compared with river DON, DIN was the dominant form of DTN, with a proportion of 88.0%. Furthermore, NO_3–N was the dominant form (88.2%) of DIN, followed by NH_4–N (9.0%), while NO_2–N had the smallest share. The mean values of water temperature, DTN, DIN, NO_3–N and ΔN_2O were significantly higher in the WJR watershed than in the NJR watershed ($p < 0.05$).

In contrast, NH_4–N was the dominant form of DIN in sediments (85.7%) and soils (83.4%), followed by NO_3–N and NO_2–N. Sediment and soil pH were significantly lower in the WJR watershed than in the NJR watershed ($p < 0.05$). However, sediment DIN, NO_2–N, and NH_4–N and soil *amo*A–AOA were significantly higher in the WJR watershed than in the NJR watershed ($p < 0.05$). Gene abundances (*amo*A–AOA, *amo*A–AOB, *nxr*A, *nar*G and *nir*S) were higher in the river than in the sediments and soils.

3.3. Relationships between land use and river nitrogen at the watershed and HSAs scales

The relationships between land use and river N obtained from the MLR model are summarized in Table 2 and Fig. 4. Spatially, at both the

Table 1
Descriptive statistics of measured parameters of river water, sediment and riparian soil in the 15 selected subwatersheds.

Parameters	Total			North Jiulong River	West Jiulong River
	Minimums	Maximums	Mean ± SD	Mean ± SD	Mean ± SD
River	*(n = 15)*			*(n = 10)*	*(n = 5)*
Temperature (°C)	22.20	27.10	23.94 ± 1.45	23.40 ± 1.05[a]	25.02 ± 1.64[b]
Conductivity (μS cm^{-1})	67.30	484.00	215.77 ± 113.95	226.29 ± 133.74	194.72 ± 66.13
pH	6.50	8.08	7.37 ± 0.51	7.52 ± 0.53	7.07 ± 0.31
DO (mg L^{-1})	4.47	10.75	8.25 ± 1.53	8.32 ± 1.80	8.12 ± 0.93
TSM (mg L^{-1})	5.86	35.00	13.45 ± 7.81	14.21 ± 8.94	11.92 ± 5.43
DTN (mg L^{-1})	1.05	14.45	4.42 ± 4.16	2.65 ± 1.17[a]	7.96 ± 5.84[b]
DON (mg L^{-1})	0.00	1.66	0.53 ± 0.51	0.37 ± 0.27	0.85 ± 0.75
DIN (mg L^{-1})	0.98	12.82	3.89 ± 3.70	2.27 ± 1.00[a]	7.11 ± 5.12[b]
NO_3–N (mg L^{-1})	0.71	12.50	3.43 ± 3.71	1.81 ± 0.84[a]	6.67 ± 5.19[b]
NO_2–N (mg L^{-1})	0.01	0.34	0.11 ± 0.10	0.11 ± 0.11	0.09 ± 0.08
NH_4–N (mg L^{-1})	0.01	1.78	0.35 ± 0.46	0.36 ± 0.54	0.34 ± 0.29
ΔN_2 (μmol L^{-1})	0.00	28.48	5.82 ± 8.04	4.98 ± 9.26	7.50 ± 5.28
ΔN_2O (nmol L^{-1})	0.00	57.70	15.28 ± 15.03	8.28 ± 7.25[a]	29.29 ± 17.45[b]
*amo*A–AOA (copies g^{-1})	2.62×10^6	1.35×10^9	$2.60 \times 10^8 \pm 4.45 \times 10^8$	$2.71 \times 10^8 \pm 5.07 \times 10^8$	$2.39 \times 10^8 \pm 3.38 \times 10^8$
*amo*A–AOB (copies g^{-1})	4.01×10^6	1.44×10^8	$3.90 \times 10^7 \pm 3.97 \times 10^7$	$4.90 \times 10^7 \pm 4.46 \times 10^7$	$1.88 \times 10^7 \pm 1.69 \times 10^7$
*nxr*A (copies g^{-1})	4.68×10^6	1.00×10^8	$3.13 \times 10^7 \pm 3.20 \times 10^7$	$3.10 \times 10^7 \pm 3.05 \times 10^7$	$3.19 \times 10^7 \pm 3.86 \times 10^7$
*nar*G (copies g^{-1})	3.40×10^8	1.69×10^{10}	$3.90 \times 10^9 \pm 4.89 \times 10^9$	$5.24 \times 10^9 \pm 5.57 \times 10^9$	$1.24 \times 10^9 \pm 7.92 \times 10^8$
*nir*S (copies g^{-1})	7.60×10^8	9.01×10^9	$3.66 \times 10^9 \pm 2.72 \times 10^9$	$4.23 \times 10^9 \pm 3.05 \times 10^9$	$2.51 \times 10^9 \pm 1.55 \times 10^9$
Sediment	*(n = 15)*			*(n = 10)*	*(n = 5)*
Moisture (%)	19.20	53.19	32.98 ± 9.66	35.30 ± 6.33	28.35 ± 14.01
pH	4.76	8.03	7.12 ± 0.81	7.48 ± 0.40[a]	6.40 ± 0.98[b]
DIN (mg kg^{-1})	11.74	109.10	32.57 ± 24.60	21.54 ± 10.34[a]	53.70 ± 31.86[b]
NO_3–N (mg kg^{-1})	2.22	10.82	4.53 ± 2.80	3.65 ± 2.72	6.11 ± 2.40
NO_2–N (mg kg^{-1})	0.02	0.35	0.13 ± 0.10	0.09 ± 0.08[a]	0.20 ± 0.11[b]
NH_4–N (mg kg^{-1})	8.70	105.53	27.91 ± 23.70	18.17 ± 8.45[a]	47.39 ± 33.07[b]
*amo*A–AOA (copies g^{-1})	1.92×10^6	7.26×10^7	$1.62 \times 10^7 \pm 1.75 \times 10^7$	$1.75 \times 10^7 \pm 2.05 \times 10^7$	$1.34 \times 10^7 \pm 1.08 \times 10^7$
*amo*A–AOB (copies g^{-1})	4.22×10^5	8.03×10^6	$2.03 \times 10^6 \pm 1.94 \times 10^6$	$2.37 \times 10^6 \pm 2.27 \times 10^6$	$1.34 \times 10^6 \pm 8.29 \times 10^5$

(*continued on next page*)

Table 1 (*continued*)

Parameters	Total			North Jiulong River	West Jiulong River
	Minimums	Maximums	Mean ± SD	Mean ± SD	Mean ± SD
*nxr*A (copies g^{-1})	2.74×10^5	1.70×10^6	$9.55 \times 10^5 \pm 4.71 \times 10^5$	$9.55 \times 10^5 \pm 4.63 \times 10^5$	$9.54 \times 10^5 \pm 5.42 \times 10^5$
*nar*G (copies g^{-1})	7.10×10^7	3.73×10^8	$1.69 \times 10^8 \pm 9.35 \times 10^7$	$1.65 \times 10^8 \pm 8.59 \times 10^7$	$1.76 \times 10^8 \pm 1.18 \times 10^8$
*nir*S (copies g^{-1})	5.71×10^7	1.06×10^9	$3.37 \times 10^8 \pm 3.06 \times 10^8$	$3.71 \times 10^8 \pm 3.55 \times 10^8$	$2.71 \times 10^8 \pm 1.89 \times 10^8$
Riparian soil	*(n = 11)*			*(n = 7)*	*(n = 4)*
Moisture (%)	9.02	23.92	16.92 ± 4.65	15.43 ± 4.85	19.52 ± 3.27
pH	4.65	8.22	6.32 ± 1.05	6.77 ± 0.86[a]	5.25 ± 0.52[b]
DIN (mg kg^{-1})	18.96	67.03	41.23 ± 15.17	37.80 ± 15.36	47.25 ± 14.82
NO_3–N (mg kg^{-1})	1.53	16.53	6.67 ± 3.74	5.26 ± 2.18	9.14 ± 4.94
NO_2–N (mg kg^{-1})	0.00	1.45	0.19 ± 0.42	0.24 ± 0.54	0.10 ± 0.02
NH_4–N (mg kg^{-1})	15.98	60.83	34.37 ± 13.73	32.30 ± 15.59	38.01 ± 10.72
*amo*A–AOA (copies g^{-1})	5.28×10^5	5.36×10^8	$1.98 \times 10^8 \pm 1.72 \times 10^8$	$1.18 \times 10^8 \pm 1.25 \times 10^{8a}$	$3.37 \times 10^8 \pm 1.63 \times 10^{8b}$
*amo*A–AOB (copies g^{-1})	1.41×10^4	4.30×10^6	$9.51 \times 10^5 \pm 1.30 \times 10^6$	$7.41 \times 10^5 \pm 1.58 \times 10^6$	$1.32 \times 10^6 \pm 5.93 \times 10^5$
*nxr*A (copies g^{-1})	3.34×10^3	2.61×10^6	$1.13 \times 10^6 \pm 8.10 \times 10^5$	$9.70 \times 10^5 \pm 8.19 \times 10^5$	$1.41 \times 10^6 \pm 8.24 \times 10^5$
*nar*G (copies g^{-1})	1.21×10^6	7.30×10^7	$3.29 \times 10^7 \pm 2.58 \times 10^7$	$4.35 \times 10^7 \pm 2.39 \times 10^7$	$1.43 \times 10^7 \pm 1.90 \times 10^7$
*nir*S (copies g^{-1})	1.72×10^5	3.89×10^8	$1.22 \times 10^8 \pm 1.13 \times 10^8$	$1.05 \times 10^8 \pm 1.24 \times 10^8$	$1.52 \times 10^8 \pm 1.00 \times 10^8$

Note: SD, standard deviation; the values marked by different lowercase letters (a and b) indicate a significant difference between the North Jiulong River and the West Jiulong River at a level of $p < 0.05$.

watershed and HSAs scales, the river dissolved nutrients (DTN and DIN) had significant positive correlations with the proportion of agricultural land ($p < 0.001$, Table 2). Specifically, at both watershed and HSAs scales, river NO_3–N had a positive correlation with the proportion of agricultural land ($p < 0.001$); river NO_2–N and NH_4–N were positively correlated with the proportion of built−up land ($p < 0.05$). For dissolved gases, $\triangle N_2O$ was positively correlated with the proportion of agricultural land ($p < 0.05$). In general, the slopes of the MLR model for DTN, DIN, NO_3–N and $\triangle N_2O$ were higher at the HSAs scale than at the watershed scale, while the slopes for NH_4–N and NO_2–N were almost the same. The value of adjusted R^2, AIC and BIC at the HSAs scale were also very close to those at the watershed scale. When time and space were considered together, the results were consistent with the results of space alone (Fig. 4).

3.4. Contribution of environmental factors to river N at the different scales

RDA summarized the contribution rate of the significant environmental factors to river N (Table 3). At both the watershed and HSAs scales, agricultural land and natural land were dominant influencing factors on river dissolved nutrients and gases, while the contribution of built−up land to the river did not reach a significant level (Table 3). Land use had no significant contribution to river denitrifier and nitrifier genes.

At the riparian zone scale, both dissolved nutrients and gases in rivers were significantly affected by sediment factors and the river internal environment (Table 3). However, both nitrifier and denitrifier genes in rivers were mainly affected by riparian soil genes (*nxr*A, *nir*S and *amo*A−AOB) and the river internal environment. No significant contributions were found in sediment factors vs. river genes or soil factors vs. river dissolved nutrients and gases.

4. Discussion

4.1. Comparing MLR models at the watershed and HSAs scales

The source of STI variation was mainly from terrain and soil environments (i.e., topographic wetness index, saturated hydraulic conductivity and soil depth) (Agnew et al., 2006). Qiu et al. (2017) indicated that the STI ranged from 3.5 to 12.6 in Fairview Farm Wildlife Preserve in north−central New Jersey, USA (area <1 km^2; elevation <300 m). In contrast, the Jiulong River watershed has a larger area (more than 14,000 km^2) and higher elevation (from 0 to 1,809 m). Thus, a relatively higher STI (from 0.4 to 31.6) was found in this study area than in previous study, which may be mainly due to the regional differences in terrain and soil conditions. The difference in geographic environment may also change the proportion of HSAs in the total area. In the present study, the HSAs of 15 selected subwatersheds were delineated based on a STI threshold value of 10, which accounted for 8.0%–17.3% of each total area (Table S1). Herron and Hairsine (1998) stated that the potential saturation areas under typical topographic and climatic conditions were less than 20% of watershed areas. This also suggested that a STI threshold value of 10 was reasonable in delineating HSAs in this study.

The relationships between land use and river N were modeled at both watershed and HSAs scales across space and time (Table 2 and Fig. 4). Giri et al. (2018) indicated that the land use within HSAs has a similar contribution to water quality (total N, total phosphorus and total suspended solids) compared with that within the watershed. Our results further indicated that this significant relationship between land use, hydrological connectivity and river N does not change with N forms. The differences of adjusted R^2, AIC and BIC were usually small between watershed and HSAs scales for river DTN, DIN, NO_3–N, NO_2–N, NH_4–N and $\triangle N_2O$ in 15 selected subwatersheds (Table 2), as well as in 5 selected subwatersheds with 3−year monitoring (Fig. 4). This suggested that, compared with the model at the watershed scale, the model at the HSAs scale had a similar performance in terms of quantifying the environmental contribution to river N.

4.2. Hydrological connectivity affects nitrogen migration at the watershed and HSAs scales

A schematic showing how hydrological connectivity affects watershed N migration is illustrated in Fig. 5a and b.

Agricultural land. In the present study, agricultural land had a significant effect ($p < 0.01$) on the concentrations of dissolved nutrients (DTN, DIN and NO_3–N) at both the watershed and HSAs scales (Table 2, Table 3 and Fig. 4). Similar results were also found in Giri et al. (2018). In particular, river NO_3–N was significantly higher in the WJR than in the NJR ($p < 0.05$, Table 1). This was mainly because the WJR

Table 2
Regression model parameters for the relationship between land use composition and river N concentration at the watershed and HSAs scales.

Group	Model items	DTN (mg L^{-1})	DIN (mg L^{-1})	NO_3–N (mg L^{-1})	NO_2–N (mg L^{-1})	NH_4–N (mg L^{-1})	$\triangle N_2O$ (nmol L^{-1})
Watershed scale	Intercept	−0.463*	−0.544**	−0.775***	0.289***	−1.492***	0.322
	Agricultural land	0.792***	0.812***	0.916***			0.651*
	Built−up land				0.860*	1.083*	
	Natural land						
	p value	0.000	0.000	0.000	0.012	0.014	0.012
	Adj. R^2	0.675	0.712	0.792	0.353	0.359	0.400
	AIC value	−48.41	−50.26	−52.92	−26.66	−22.66	−40.03
	BIC value	−46.99	−48.84	−51.50	−25.24	−21.25	−38.62
HSAs scale	Intercept	−1.348**	−1.425**	−1.731***	−1.905***	−1.642**	−0.373
	Agricultural land	1.272***	1.285***	1.438***			1.025*
	Built−up land				0.782*	0.941*	
	Natural land						
	p value	0.000	0.000	0.000	0.026	0.038	0.021
	Adj. R^2	0.605	0.620	0.678	0.275	0.254	0.340
	AIC value	−45.52	−46.07	−46.37	−24.95	−20.38	−38.60
	BIC value	−44.10	−44.66	−44.95	−23.53	−18.96	−37.18

Note: All measured data in November of 2018 (n = 15) were converted by logarithm method before regression analysis; HSAs, hydrologically sensitive areas; Adj. R^2, adjusted determination coefficient; AIC, Akaike information criterion; BIC, Bayesian information criterion; *, $p < 0.05$; **, $p < 0.01$; ***, $p < 0.001$.

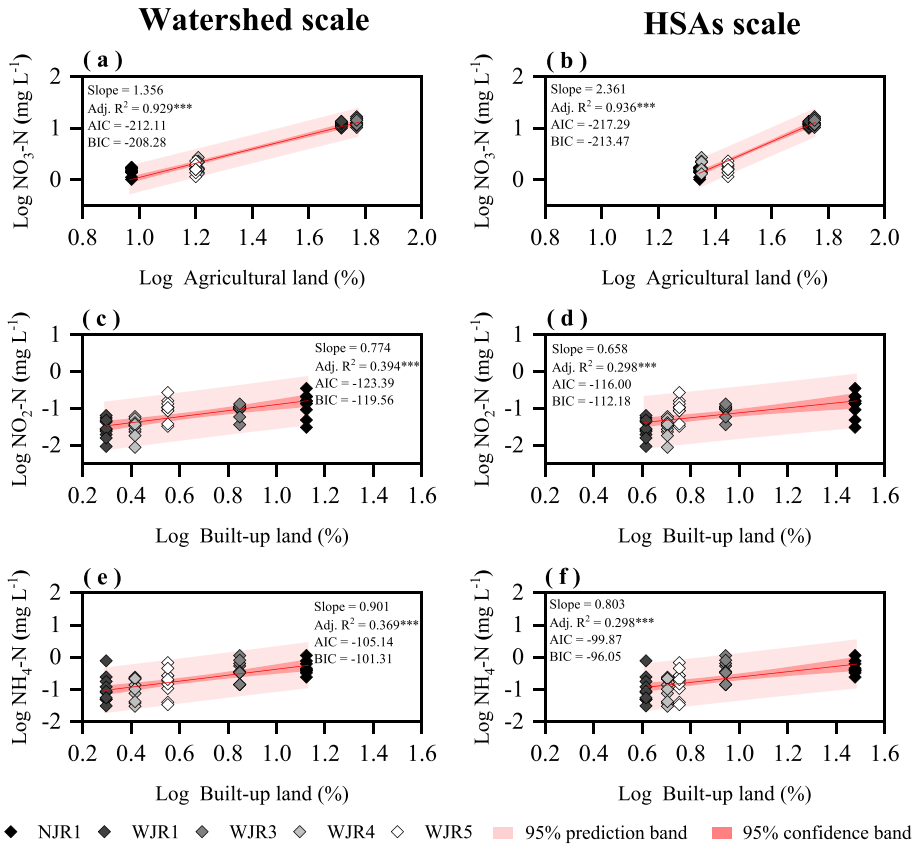

Fig. 4. Relationships between land use and river N at the watershed and HSAs scales during 2017–2019 (n = 50). HSAs, hydrologically sensitive areas; Adj. R^2, adjusted determination coefficient; AIC, Akaike information criterion; BIC, Bayesian information criterion; ***, $p < 0.001$.

watershed was a typical agricultural watershed (Fig. 3). A large amount of ammonia fertilizer was applied to agricultural land, which caused serious NO_3–N (from nitrification) pollution in the water environment of the watershed (Chen et al., 2015). Thus, NO_3–N also became the dominant form for DIN and DTN (Table 1). The HSAs represented the areas that were most likely to produce runoff in a watershed (Thomas et al., 2016). In particular, the negative charged NO_3–N tends to move with water flow (Sith et al., 2019; Zhu et al., 2018). Therefore, the slope of the MLR model was higher at the HSAs scale than at the watershed scale across time and space (Table 2 and Fig. 4). This also implies that HSAs maybe the main channel (pathway) of surface export for NO_3–N in agricultural watersheds.

In addition to dissolved nutrients, Weitz et al. (2001) stated that soil moisture and agricultural fertilization drove the release of N_2O. This was also supported by Chen et al. (2020), who proposed that agricultural land had high greenhouse gas emissions from farming inputs and operations in the WJR watershed. In this study, agricultural land had a significant positive correlation with river $\triangle N_2O$ at both the watershed and HSAs scales ($p < 0.05$, Table 2). In particular, the increase in agricultural land within HSAs had a greater impact (higher slope in the MLR model) on the release of river N_2O than it did within the watershed. On the one hand, this may be attributed to HSAs transporting a large

Table 3
The contribution rate of environment parameters to river dissolved nutrients, dissolved gases, nitrifier genes and denitrifier genes at different scale based on redundancy analysis.

Scale	Components	Dissolved nutrients		Dissolved gases		Nitrifier genes		Denitrifier genes	
		Parameter	Contribution (%)	Parameter	Contribution (%)	Parameter	Contribution (%)	Parameter	Contribution (%)
Watershed scale	Land use	Natural land	71**	Natural land	27*				
		Agricultural land	70**	Agricultural land	24*				
HSAs scale	Land use	Agricultural land	65**	Agricultural land	23*				
		Natural land	50**	Natural land	19*				
Riparian scale	River	Temperature	58**	DIN	33*	*nirS*	55**	*amo*A–AOB	41**
		ΔN_2O	39*	DTN	33*	*narG*	31*	*nxr*A	36*
				Temperature	32*			*amo*A–AOA	34*
				NO_3–N	30*				
				DON	26*				
				DO	24*				
	Sediment	pH	45**	NO_3–N	45**				
	Soil					*amo*A–AOB	44*	*amo*A–AOB	33*
						nirS	38*		
						*nxr*A	34*		

Note: Measured parameters related to river N are classified into four categories, i.e. dissolved nutrients, dissolved gases, nitrifier genes and denitrifier genes. River dissolved nutrients include DTN, DON, DIN, NO_3–N, NO_2–N and NH_4–N; dissolved gases include ΔN_2O and ΔN_2; nitrifier genes include *amo*A–AOA, *amo*A–AOB and *nxr*A; denitrifier genes include *nar*G and *nir*S. Here, only the results of redundancy analysis with statistical significance are listed. Specific ordination plots of redundancy analysis refer to Fig. S3 and Fig. S4. HSAs, hydrologically sensitive areas; * and ** indicate significant at the level of $p < 0.05$ and $p < 0.01$, respectively.

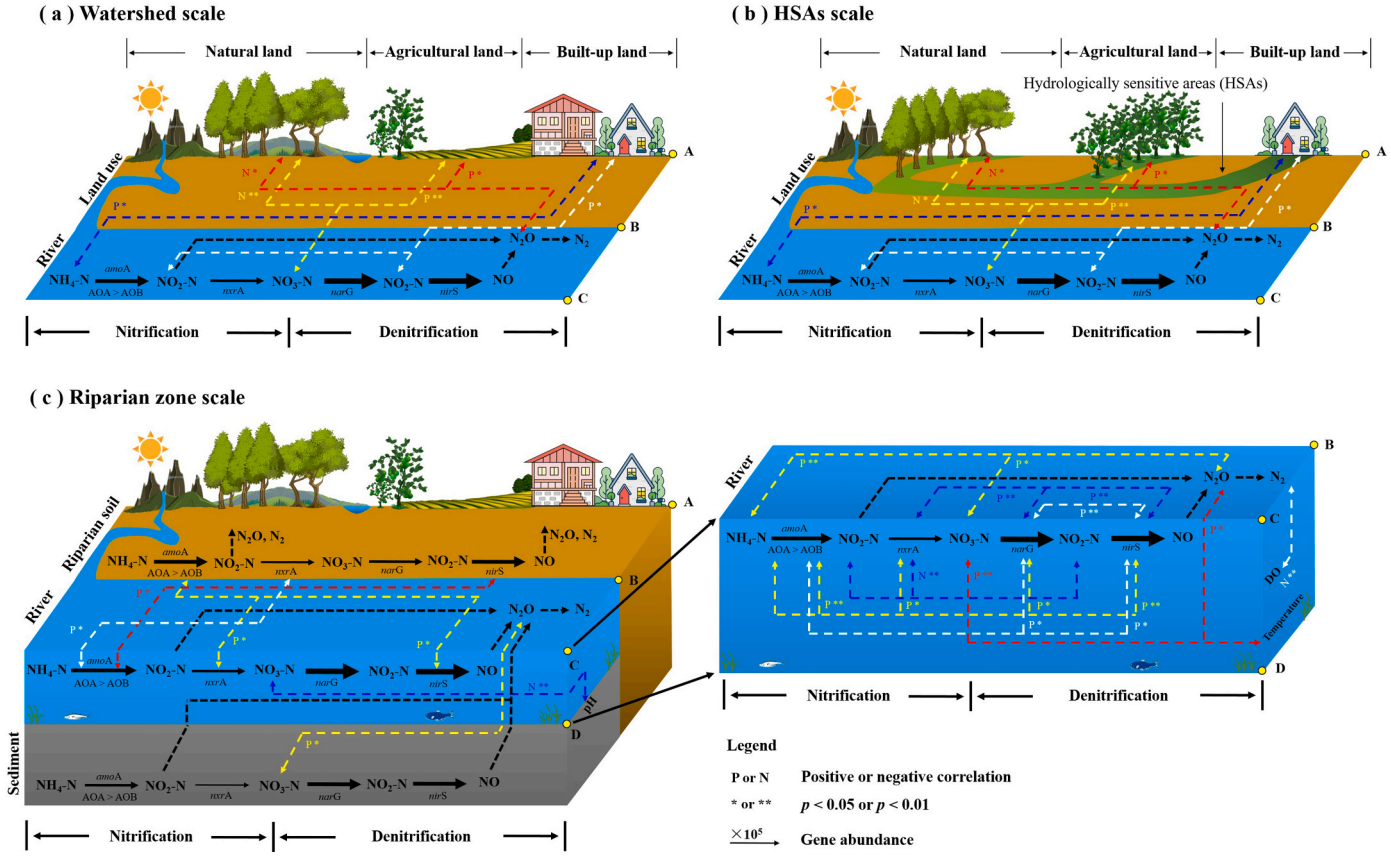

Fig. 5. A schematic showing hydrological connectivity affects nitrogen migration and retention in the land–river continuum.

amount of N into river, which provide sufficient substrates for nitrification and denitrification processes. On the other hand, HSAs usually have high soil moisture (Giri et al., 2018). Previous study indicated that soil moisture has a significant positive correlation to the growth of ammonia oxidiser and denitrifier communities (Di et al., 2014). This may also promote the release of N_2O in HSAs and river by nitrification and denitrification processes. Our results also indicated that river NH_4–N ($p < 0.01$) and NO_3–N ($p < 0.05$) had a significant positive correlation with river N_2O (Fig. 5c). Significantly higher river NO_3–N and $\triangle N_2O$ were found in the WJR than in the NJR ($p < 0.05$, Table 1). This implied that intensive agricultural watersheds export a large quantity of N along HSAs and further change river N retention by the

release of N_2O.

Built−up land. Previous studies have shown that river NH_4–N was primarily comes from surface land and transported by overland flow in rainstorm events (Mihiranga et al., 2021). Especially, in built−up land, the discharge of both raw/treated sewage and livestock wastewater greater increased the concentration of NH_4–N in the river (Lin et al., 2020b). NO_2–N is an intermediate product during the process of nitrification and denitrification and is closely related to NH_4–N (Abbas et al., 2020; Lin et al., 2020b). Cao et al. (2015) used N isotopes ($\delta^{15}N$) to reveal that NH_4–N mainly came from the urban section, especially in the upper reaches of the NJR (Longyan city and suburban area). In this study, NH_4–N and NO_2–N were significantly correlated with built−up land (Table 2 and Fig. 4). The NJR watershed has a higher percentage of built−up land than the WJR watershed, especially at the HSAs scale (Fig. 3). However, the built−up land at the HSAs and watershed scales contributes similarly to the river NH_4–N and NO_2–N across both time and space (Table 2 and Fig. 4). This indicates that reducing built−up land or improving wastewater treatment within HSAs is expected to improve river quality (reduce ammonium loading).

Natural land. Natural land (e.g., forestland, grassland and wetland) is usually less disturbed by human activities. In this study, natural land had significant contributions to the concentrations of dissolved nutrients and gases in the rivers (Table 3). A significant negative correlation was also found in natural land vs. river NO_3–N and N_2O (Fig. 5a and b). Our results indicated that an increase in natural land has a high potential to reduce river N loading and to improve water quality. This was supported by Giri et al. (2017), who stated that one percent increase in forestland could reduce the concentration of stream N by 0.039 ppm in north−central New Jersey, USA. In addition, grasslands significantly reduce N_2O emissions compared with farmlands and orchards (Wang et al., 2020a). Wetlands usually have a high denitrification and anammox potential with a strong capacity for N removal due to their low oxygen and high organic carbon content (Wang et al., 2019). Therefore, ecological restoration from agricultural land and built−up land in HSAs to natural land should be given priority to improve water quality.

4.3. Hydrological connectivity affects river nitrogen retention at the riparian zone scale

A schematic showing how hydrological connectivity affects river N retention processes is illustrated in Fig. 5c.

River and soil. The riparian zone is the final delivery zone of nutrients along HSAs. These nutrients entering the river could stimulate microbe−driven nitrification and denitrification. In general, river microorganisms attaching to particles could come from three main sources (Miller et al., 2014; Zaimes et al., 2021): (1) soil erosion and sediment suspension from the upper river; (2) soil erosion near the riverbank; and (3) the resuspension of river sediment. In this study, compared with sediment, nitrification and denitrification genes in river water were significantly correlated with riparian soil genes ($p < 0.05$ and $p < 0.01$, respectively, Table 3). This implied that the functional genes in rivers mainly originated from the adjacent lands. Zaimes et al. (2021) suggested that steep sloped land exacerbates soil erosion in a watershed. Long−term farming, heavy rainfall and mountainous terrain were summarized as the main causes of severe soil erosion in the hilly red soil region of southern China (Wang et al., 2020b). Furthermore, the riparian soil DIN and functional genes under agricultural land were higher than under natural land, although the differences were not significant (Table S3). Soil erosion and external nutrients entering river channels along HSAs may have stimulated nitrogen retention processes in the river water and sediments.

River and sediment. Our results showed that the concentrations of dissolved nutrients and gases in rivers were significantly correlated with sediment and river water factors (Table 3). In addition to external inputs, the mineralization of organic N within river channels is another source of river NH_4–N (Lin et al., 2019). The availability of oxygen in river water and surface sediments favors nitrification and the conversion of NH_4–N to NO_3–N (Zhu et al., 2021). However, nitrification may be relatively weak in anaerobic sediments compared with that in river water, as evidenced by a low abundance of nitrification genes (*amo*A−AOA, *amo*A−AOB and *nxr*A) in sediments (Table 1). River NO_3–N diffuses into the sediments, followed by denitrification and the release of N_2O into the overlying water. In some turbid rivers, the high content of river particles forms local anaerobic conditions that favor denitrification (Yang et al., 2021; Zhou et al., 2019). Our results also suggested that the NO_3–N in both river water and sediments had a significant positive correlation with river N_2O ($p < 0.05$, Fig. 5c). Meanwhile, a significant ($p < 0.05$) negative correlation was found between sediment pH and river NO_3–N in this study (Fig. 5c). In particular, soil and sediment pH were significantly lower in the WJR (an agricultural watershed) than in the NJR (Table 1). This was mainly because the long−term overuse of N fertilizer has resulted in severe NO_3–N pollution as well as soil acidification (low pH), while the low pH significantly increased the emission ratio of $N_2O/(N_2O + N_2)$ from soils and sediments (Qu et al., 2014; Russenes et al., 2016). These results suggested that hydrological connectivity affected river N retention processes, and controlling fertilizers in agricultural watersheds is urgently needed to reduce N_2O release.

4.4. Implications for watershed management

The management strategies of watershed nutrients are illustrated in Fig. 6. HSAs cover less than 20% of the watershed area, which play an important role in transporting land N into river channels. Given the relationship between land use and river N, we recommend reducing the area of agricultural land (in the WJR watershed) and built−up land (in the NJR watershed) in HSAs and converting them to natural land to improve water quality (reduce river N concentration). In the riparian zone, soil erosion and sediment denitrification were found to be among the important factors affecting river retention processes (i.e., nitrification and denitrification). In view of this, natural land (e.g., forestland, grassland and wetland) is necessary in riparian buffer strips to control soil erosion. Moreover, reducing N fertilizer application on agricultural land is expected to reduce greenhouse gas N_2O emissions.

Previous studies have provided valuable insights into watershed nutrient management. For example, Thomas et al. (2016) suggested that targeting riparian buffer strips at HSAs delivery points would reduce costs. Hui et al. (2021) revealed that the specific flow structure of channel confluences created a distinctive context with a long hydraulic retention time, which promoted microbial growth and N removal. Chen et al. (2017) suggested that the multipond system was beneficial in intercepting pollutants. Thus, setting up a multipond system near HSAs and targeting HSAs delivery points and river channel confluences could efficiently improve water quality compared with watershed−wide management practices (Fig. 6).

The detailed design of applicable measures to restore river ecosystems was beyond the scope of the present study, but future efforts should be made to develop a systematic cost−benefit analysis. In addition, a watershed−scale biogeochemical model coupled with an economical model is necessary to quantify the linkage between the implementation of management practices and the improvement of water quality in river networks. Especially, HSAs represent the areas that are most likely to produce surface runoff with a relatively wet soil condition (Buchanan et al., 2014; Giri et al., 2018). Potentially, the subsurface (e.g., soil interflow and groundwater flow) of these areas may also have strong hydraulic transport capacity to regulate the migration and transformation of watershed N. Meanwhile, the climate change (e.g., extreme rainstorm events) and human activities (e.g., drainage networks) may change the path of the water flow (hydrological connectivity), which should also be incorporated into future researches.

4.5. Uncertainty analysis

Some limitations were involved in this study. (1) Thomas et al.

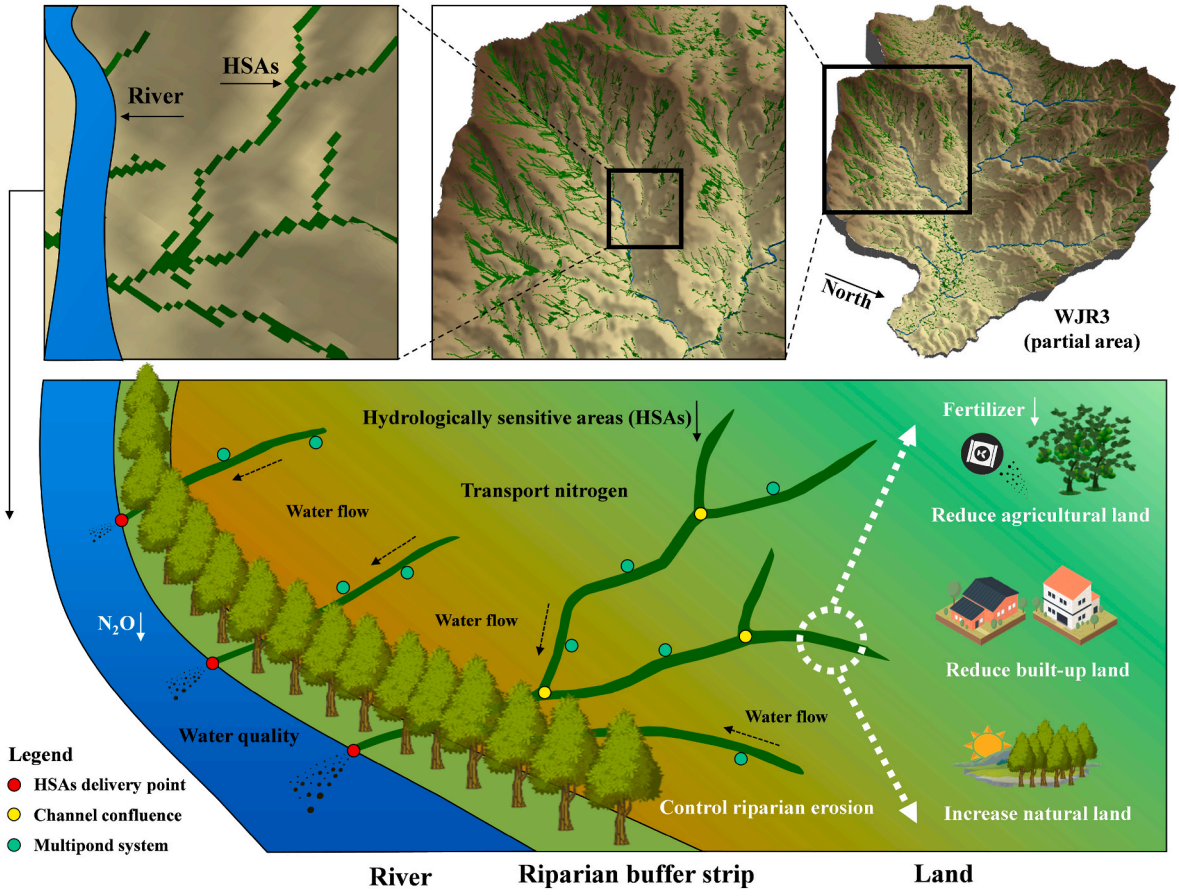

Fig. 6. A schematic showing the management strategies of watershed nitrogen.

(2017) indicated that a LiDAR DEM of 1–2 m is optimal for HSAs modeling. However, such fine topography is difficult to obtain at large scales. In this study, a DEM of 12.5 m spatial resolution is relatively appropriate due to the watershed area more than 10,000 km^2. (2) This study refers to previous researches and uses an experience value (STI = 10) to delineate HSAs in the watershed. Currently, there is still no unified standard to determine the threshold value of STI for a specific watershed. More researches are needed to reduce these uncertainties.

5. Conclusions

This study explored the role of hydrological connectivity on N migration and retention in the land–river continuum. HSAs occupied a small area (8.0%–17.3%) of the watershed, but their land use pattern explains river N variations, which is equivalent to watershed land use. HSAs are hotspots for transporting land N into river channels. In particular, in the HSAs, agricultural land exported more NO_3–N and promoted the release of N_2O, while built–up land mainly contributed NH_4–N and NO_2–N to the rivers. Riparian soil erosion and sediment denitrification were found to be among the most important factors affecting river N retention processes (i.e., nitrification and denitrification). Therefore, controlling fertilizer use and sewage discharge, converting agricultural land and built–up land to natural land in HSAs, and avoiding soil erosion in HSAs and riparian zones are expected to efficiently reduce watershed N loading and improve river water quality.

Credit author statement

YaoWang: Writing–original draft, Data curation, Methodology, Visualization, Formal analysis. **Jingjie Lin:** Investigation, Data curation, Formal analysis. **Fenfang Wang:** Data curation, Formal analysis. **Qing Tian:** Investigation, Data curation. **Yi Zheng:** Software, Conceptualization. **Nengwang Chen:** Writing–review & editing, Conceptualization, Supervision, Resources.

Declaration of competing interest

The authors declare that they have no known competing financial interests or personal relationships that could have appeared to influence the work reported in this paper.

Data availability

Data will be made available on request.

Acknowledgments

This research was supported by the National Natural Science Foundation of China (No. 51961125203) and the Fujian Province Water Conservancy Science and Technology Project. We thank Dr. Samuel Smidt and two anonymous reviewers for their constructive suggestions that improved the manuscript. We thank Junou Du, Xiuxiu Wang, Zeyang Lu, Minxiang Zhu, Xin Yuan, Yan Fang, Weijie Gong and all peoples who assisted in field investigation and lab analysis. We thank to Prof. Shaobin Li from Xiamen University for his insightful comments.

Appendix A. Supplementary data

Supplementary data to this article can be found online at https://doi.org/10.1016/j.jenvman.2022.116816.

References

Abbas, T., Zhang, Q., Zou, X., Tahir, M., Wu, D., Jin, S., Di, H., 2020. Soil anammox and denitrification processes connected with N cycling genes co–supporting or contrasting under different water conditions. Environ. Int. 140, 105757.

Agnew, L.J., Lyon, S.W., Gerard–Marchant, P., Collins, V.B., Lembo, A.J., Steenhuis, T.S., Walter, M.T., 2006. Identifying hydrologically sensitive areas: bridging the gap between science and application. J. Environ. Manag. 78 (1), 63–76.

Anderson, T.R., Goodale, C.L., Groffman, P.M., Walter, M.T., 2014. Assessing denitrification from seasonally saturated soils in an agricultural landscape: a farm–scale mass–balance approach. Agric. Ecosyst. Environ. 189, 60–69.

Anderson, T.R., Groffman, P.M., Walter, M.T., 2015. Using a soil topographic index to distribute denitrification fluxes across a northeastern headwater catchment. J. Hydrol. 522, 123–134.

Bossolani, J.W., Crusciol, C.A.C., Merloti, L.F., Moretti, L.G., Costa, N.R., Tsai, S.M., Kuramae, E.E., 2020. Long–term lime and gypsum amendment increase nitrogen fixation and decrease nitrification and denitrification gene abundances in the rhizosphere and soil in a tropical no–till intercropping system. Geoderma 375, 11476.

Buchanan, B.P., Fleming, M., Schneider, R.L., Richards, B.K., Archibald, J., Qiu, Z., Walter, M.T., 2014. Evaluating topographic wetness indices across central New York agricultural landscapes. Hydrol. Earth Syst. Sci. 18 (8), 3279–3299.

Cao, W.Z., Huang, Z., Zhai, W.D., Li, Y., Hong, H.S., 2015. Isotopic evidence on multiple sources of nitrogen in the northern jiulong River, Southeast China. Estuar. Coast Shelf Sci. 163, 37–43.

Chen, N., Chen, Z., Wu, Y., Hu, A., 2014. Understanding gaseous nitrogen removal through direct measurement of dissolved N_2 and N_2O in a subtropical river–reservoir system. Ecol. Eng. 70, 56–67.

Chen, N., Wu, J., Zhou, X., Chen, Z., Lu, T., 2015. Riverine N_2O production, emissions and export from a region dominated by agriculture in Southeast Asia (Jiulong River). Agric. Ecosyst. Environ. 208, 37–47.

Chen, Q., Guo, X., Hua, G., Li, G., Feng, R., Liu, X., 2017. Migration and degradation of swine farm tetracyclines at the river catchment scale: can the multi–pond system mitigate pollution risk to receiving rivers? Environ. Pollut. 220, 1301–1310.

Chen, X., Xu, X., Lu, Z., Zhang, W., Yang, J., Hou, Y., Wang, X., Zhou, S., Li, Y., Wu, L., Zhang, F., 2020. Carbon footprint of a typical pomelo production region in China based on farm survey data. J. Clean. Prod. 277, 124041.

Di, H.J., Cameron, K.C., Podolyan, A., Robinson, A., 2014. Effect of soil moisture status and a nitrification inhibitor, dicyandiamide, on ammonia oxidizer and denitrifier growth and nitrous oxide emissions in a grassland soil. Soil Biol. Biochem. 73, 59–68.

Fischer, R.A., Fischenich, J.C., 2000. Ecosystem Management and Restoration Research Program. In: Design Recommendations for Riparian Corridors and Vegetated Buffer Strips. U.S. Army Corps of Engineers.

Fox, G.A., Purvis, R.A., Penn, C.J., 2016. Streambanks: a net source of sediment and phosphorus to streams and rivers. J. Environ. Manag. 181, 602–614.

Giri, S., Qiu, Z.Y., Zhang, Z., 2017. A novel technique for establishing soil topographic index thresholds in defining hydrologically sensitive areas in landscapes. J. Environ. Manag. 200, 391–399.

Giri, S., Qiu, Z.Y., Zhang, Z., 2018. Assessing the impacts of land use on downstream water quality using a hydrologically sensitive area concept. J. Environ. Manag. 213, 309–319.

Hansen, A., Campbell, T., Cho, S., Czuba, J., Dalzell, B., Dolph, C., Hawthorne, P., Rabotyagov, S., Lang, Z., Kumarasamy, K., Belmont, P., Finlay, J., Foufoula–Georgiou, E., Gran, K., Kling, C., Wilcock, P., 2021. Integrated assessment modeling reveals near–channel management as cost–effective to improve water quality in agricultural watersheds. P. Natl. Acad. Sci. USA. 118 (28), 1–8.

Herron, N.F., Hairsine, P.B., 1998. A scheme for evaluating the effectiveness of riparian zones in reducing overland flow to streams. Aust. J. Soil Res. 36 (4), 683–698.

Hui, C., Li, Y., Zhang, W., Yang, G., Wang, H., Gao, Y., Niu, L., Wang, L., Zhang, H., 2021. Coupling genomics and hydraulic information to predict the nitrogen dynamics in a channel confluence. Environ. Sci. Technol. 55 (8), 4616–4628.

Hurvich, C.M., Simonoff, J.S., Tsai, C.L., 1998. Smoothing parameter selection in nonparametric regression using an improved Akaike information criterion. J. R. Stat. Soc. B–Statistical Methodology 60, 271–293.

Lehnert, N., Musselman, B.W., Seefeldt, L.C., 2021. Grand challenges in the nitrogen cycle. Chem. Soc. Rev. 50 (6), 3640–3646.

Li, S., Cai, X., Seyed, A.E., Ankita, J., Sundar, N., Seojeong, O., Kevin, W., Roland, D.C., Benjamin, M.G., Stephen, J., Gregory, F.M., Vijay, S., 2021. Developing an integrated technology–environment–economics model to simulate food–energy–water systems in Corn Belt watersheds. Environ. Model. Software 143, 105083.

Lin, J.L. (Ed.), 1991. Fujian Soil. Fujian Science and Technology Press (Fujian), pp. 69–214 (in Chinese).

Lin, J., Chen, N., Wang, F., Huang, Z., Zhang, X., Liu, L., 2020a. Urbanization increased river nitrogen export to western Taiwan Strait despite increased retention by nitrification and denitrification. Ecol. Indicat. 109, 105756.

Lin, J., Chen, N., Yuan, X., Tian, Q., Hu, A., Zheng, Y., 2020b. Impacts of human disturbance on the biogeochemical nitrogen cycle in a subtropical river system revealed by nitrifier and denitrifier genes. Sci. Total Environ. 746, 141139.

Lin, J., Tang, Y., Liu, D., Zhang, S., Lan, B., He, L., Yu, Z., Zhou, S., Chen, X., Qu, Y., 2019. Characteristics of organic nitrogen fractions in sediments of the water level fluctuation zone in the tributary of the Yangtze River. Sci. Total Environ. 653, 327–333.

Lutz, S.R., Trauth, N., Musolff, A., Van Breukelen, B.M., Knöller, K., Fleckenstein, J.H., 2020. How important is denitrification in riparian zones? Combining end–member mixing and isotope modeling to quantify nitrate removal from riparian groundwater. Water Resour. Res. 56 (1), 1–26.

Mihiranga, H.K.M., Jiang, Y., Li, X., Wang, W., Silva, K.D., Kumwimba, M.N., Bao, X., Nissanka, S.P., 2021. Nitrogen/phosphorus behavior traits and implications during storm events in a semi–arid mountainous watershed. Sci. Total Environ. 791 (1), 148382.

Miller, R.B., Fox, G.A., Penn, C.J., Wilson, S., Parnell, A., Purvis, R.A., Criswell, K., 2014. Estimating sediment and phosphorus loads from streambanks with and without riparian protection. Agric. Ecosyst. Environ. 189, 70–81.

Qiu, Z., Pennock, A., Giri, S., Trnka, C., Du, X., Wang, H., 2017. Assessing soil moisture patterns using a soil topographic index in a humid region. Water Resour. Maneg. 31 (7), 2243–2255.

Qiu, Z.Y., Kennen, J.G., Giri, S., Walter, T., Kang, Y., Zhang, Z., 2019. Reassessing the relationship between landscape alteration and aquatic ecosystem degradation from a hydrologically sensitive area perspective. Sci. Total Environ. 650, 2850–2862.

Qu, Z., Wang, J., Almoy, T., Bakken, L.R., 2014. Excessive use of nitrogen in Chinese agriculture results in high $N_2O/(N_2O+N_2)$ product ratio of denitrification, primarily due to acidification of the soils. Global Change Biol. 20 (5), 1685–1698.

Russenes, A.L., Korsaeth, A., Bakken, L.R., Dorsch, P., 2016. Spatial variation in soil pH controls off–season N_2O emission in an agricultural soil. Soil Biol. Biochem. 99, 36–46.

Shrewsbury, L.H., Smith, J.L., Huggins, D.R., Carpenter–Boggs, L., Reardon, C.L., 2016. Denitrifier abundance has a greater influence on denitrification rates at larger landscape scales but is a lesser driver than environmental variables. Soil Biol. Biochem. 103, 221–231.

Sith, R., Watanabe, A., Nakamura, T., Yamamoto, T., Nadaoka, K., 2019. Assessment of water quality and evaluation of best management practices in a small agricultural watershed adjacent to Coral Reef area in Japan. Agric. Water Manag. 213, 659–673.

Song, X.P., Hansen, M.C., Stehman, S.V., Potapov, P.V., Tyukavina, A., Vermote, E.F., Townshend, J.R., 2018. Global land change from 1982 to 2016. Nature 560 (7720), 639–643.

Tang, Y., Yu, G., Zhang, X., Wang, Q., Tian, D., Tian, J., Niu, S., Ge, J., 2019. Environmental variables better explain changes in potential nitrification and denitrification activities than microbial properties in fertilized forest soils. Sci. Total Environ. 647, 653–662.

Thomas, I.A., Jordan, P., Mellander, P.E., Fenton, O., Shine, O., Huallachain, D.O., Creamer, R., McDonald, N.T., Dunlop, P., Murphy, P.N.C., 2016. Improving the identification of hydrologically sensitive areas using LiDAR DEMs for the delineation and mitigation of critical source areas of diffuse pollution. Sci. Total Environ. 556, 276–290.

Thomas, I.A., Jordan, P., Shine, O., Fenton, O., Mellander, P.E., Dunlop, P., Murphy, P.N.C., 2017. Defining optimal DEM resolutions and point densities for modelling hydrologically sensitive areas in agricultural catchments dominated by microtopography. Int. J. Appl. Earth Obs. 54 38–52.

van-Lent, J., Hergoualc'h, K., Verchot, L.V., 2015. Reviews and syntheses: soil N_2O and NO emissions from land use and land–use change in the tropics and subtropics: a meta–analysis. Biogeosciences 12 (23), 7299–7313.

Walter, M.T., Walter, M.F., Brooks, E.S., Steenhuis, T.S., Boll, J., Weiler, K., 2000. Hydrologically sensitive areas: variable source area hydrology implications for water quality risk assessment. J. Soil Water Conserv. 55 (3), 277–284.

Wang, F., Chen, N., Yan, J., Lin, J., Guo, W., Cheng, P., Liu, Q., Huang, B., Tian, Y., 2019. Major processes shaping mangroves as inorganic nitrogen sources or sinks: insights from a multidisciplinary study. J Geophys Res–Biogeo. 124, 1194–1208.

Wang, H., Shu, D., Liu, D., Liu, S., Deng, N., An, S., 2020a. Passive and active ecological restoration strategies for abandoned farmland leads to shifts in potential soil nitrogen loss by denitrification and soil denitrifying microbes. Land Degrad. Dev. 31 (9), 1086–1098.

Wang, L., Yan, H., Wang, X.W., Wang, Z., Yu, S.X., Wang, T.W., Shi, Z.H., 2020b. The potential for soil erosion control associated with socio–economic development in the hilly red soil region, southern China. Catena 194, 104678.

Wang, Y., Xiao, Z., Aurangzeib, M., Zhang, X., Zhang, S., 2021. Effects of freeze–thaw cycles on the spatial distribution of soil total nitrogen using a geographically weighted regression kriging method. Sci. Total Environ., 142993

Weitz, A.M., Linder, E., Frolking, S., Crill, P.M., Keller, M., 2001. N_2O emissions from humid tropical agricultural soils: effects of soil moisture, texture and nitrogen availability. Soil Biol. Biochem. 33 (7–8), 1077–1093.

Willett, C.D., Lerch, R.N., Schultz, R.C., Berges, S.A., Peacher, R.D., Isenhart, T.M., 2012. Streambank erosion in two watersheds of the central claypan region of Missouri, United States. J. Soil Water Conserv. 67 (4), 249–263.

Xiong, R., Zheng, Y., Chen, N.W., Tian, Q., Liu, W., Han, F., Jiang, S.J., Lu, M.Q., Zheng, Y., 2022. Predicting dynamic riverine nitrogen export in unmonitored watersheds: leveraging insights of AI from data–rich regions. Environ. Sci. Technol. 56 (14), 10530–10542.

Yang, D., Wang, D., Chen, S., Ding, Y., Gao, Y., Tian, H., Cai, R., Yu, L., Deng, H., Chen, Z., 2021. Denitrification in urban river sediment and the contribution to total nitrogen reduction. Ecol. Indicat. 120, 106960.

Zaimes, G., Tamparopoulos, A.E., Tufekcioglu, M., Schultz, R.C., 2021. Understanding stream bank erosion and deposition in Iowa, USA: a seven year study along streams in different regions with different riparian land–uses. J. Environ. Manag. 287, 112352.

Zhao, S., Zhang, B., Sun, X., Yang, L., 2021. Hot spots and hot moments of nitrogen removal from hyporheic and riparian zones: a review. Sci. Total Environ. 762, 144168.

Zhou, Y., Xu, X., Han, R., Li, L., Feng, Y., Yeerken, S., Song, K., Wang, Q., 2019. Suspended particles potentially enhance nitrous oxide (N_2O) emissions in the oxic

estuarine waters of eutrophic lakes: field and experimental evidence. Environ. Pollut. 252, 1225–1234.
Zhu, L., Shi, W., Zhou, J., Yu, J., Kong, L., Qin, B., 2021. Strong turbulence accelerates sediment nitrification–denitrification for nitrogen loss in shallow lakes. Sci. Total Environ. 761, 143210.
Zhu, Q., Castellano, M.J., Yang, G., 2018. Coupling soil water processes and the nitrogen cycle across spatial scales: potentials, bottlenecks and solutions. Earth Sci. Rev. 187, 248–258.